

SALTATION THRESHOLD AND IMPACT RIPPLE DYNAMICS DOWN TO MARTIAN PRESSURE AND BELOW. B. Andreotti¹, P. Claudin², J.J. Iversen³, J.P. Merrison³ and K.R. Rasmussen^{3,4}, ¹Laboratoire de Physique de l'Ecole Normale Supérieure, CNRS - Université de Paris - PSL Research University, 75005 Paris, France, ²Physique et Mécanique des Milieux Hétérogènes, CNRS - ESPCI Paris - PSL Research University - Sorbonne Université - Université de Paris, 75005 Paris, France (philippe.claudin@espci.fr), ³Department of Physics and Astronomy, Aarhus University, 8000 Aarhus C, Denmark, ⁴Department of Geoscience, Aarhus University, 8000 Aarhus C, Denmark.

Introduction: Aeolian sediment transport is observed to occur on Mars as well as in other extraterrestrial environments, generating ripples and dunes as on Earth [1,2,3]. The search for terrestrial analogues of planetary bedforms, as well as environmental simulation experiments able to reproduce their formation in planetary conditions, are powerful ways to question our understanding of geomorphological processes towards unusual environmental conditions. Here, we briefly report sediment transport laboratory experiments performed in a closed-circuit wind tunnel placed in a vacuum chamber and operated at extremely low pressures (Fig. 1). Full details on experimental set-up and data analysis can be found in [4].

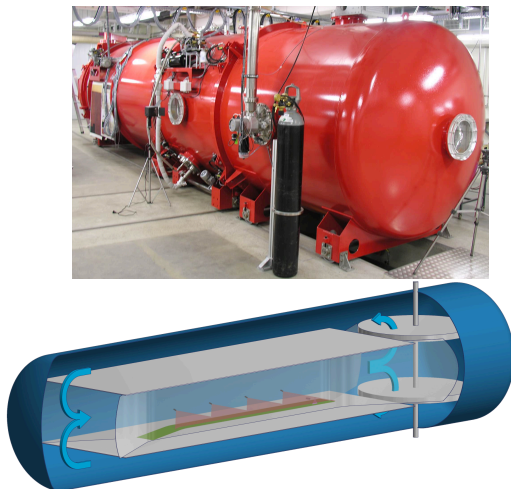


Fig. 1: Photo (top) and schematics (bottom) of the tunnel. Length of working section: 3.25 m.

Saltation threshold: The determination of the threshold wind speed below which no sediment transport occurs is an old problem, but is still currently investigated for various environments, see e.g. [5]. Previous data in low-pressure conditions show sensitivity of the threshold measurements with particle size [6,7]. In our experiments, the grain size is fixed but we systematically vary the pressure (i.e. air density ρ_f) over three orders of magnitude. We use a long-distance microscope to measure the number of moving

grains in a control volume located close to the bed as a function of time. With increasing wind speed one observes a transition from a regime of individual grains transported intermittently due to turbulent fluctuations to a regime with bursts composed of a number of moving particles that is rapidly increasing with the shear velocity. The threshold can be defined by extrapolating to zero the average number of grains per burst (Fig. 2 top).

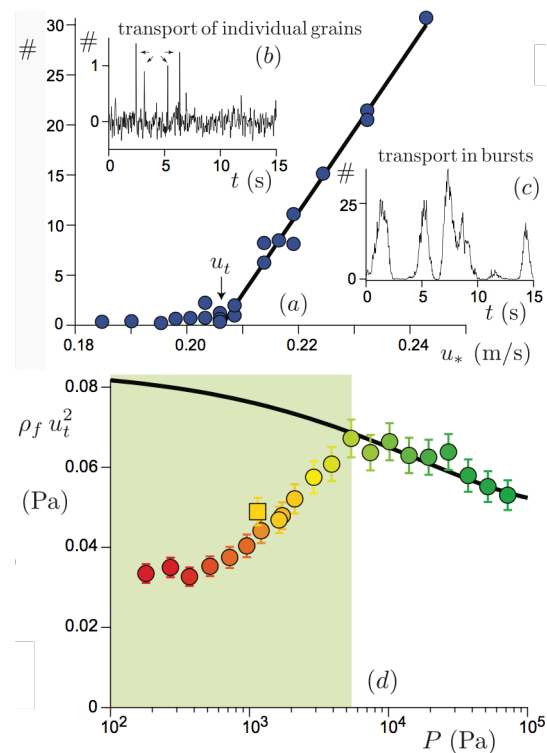


Fig. 2: Number of moving grains in a controlled volume at different flow velocity (top). Variation of the stress threshold with air pressure in the tunnel (bottom). New regime in green.

At relatively high pressures (up to a density ratio between grain and air of about 4×10^5), our results follow the prediction of a 'dynamic' threshold model adjusted in the ambient conditions. It accounts both for the transition from Stokes to turbulent drag as determined by the grain Reynolds number, and for the

transition from a rough to a smooth (viscous) boundary layer [4]. At low pressures, however, the measured threshold gradually deviates from this expected theoretical law, providing experimental evidence of a previously unexplored regime, which includes Martian conditions, and cannot be explained by these hydrodynamic transitions (Fig. 2 bottom).

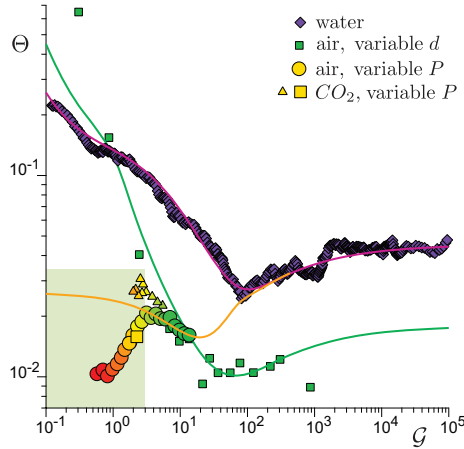


Fig. 3: Transport threshold in the dimensionless plane Shields vs Galileo numbers. The symbols' color codes for the density ratio, i.e. the pressure (Fig. 2 bottom).

To compare sediment transport in various conditions, one must identify the relevant dimensionless numbers. The shear velocity u_* can be rescaled using the grain size d and the fluid density to form the Shields number $\Theta = \rho_f u_*^2 / (\rho_p - \rho_f) g d$ which compares the fluid shear stress exerted on the particles to their apparent weight. Neglecting cohesion, its threshold value associated with the incipient motion of particles at the surface of a static bed only depends on a the Galileo number $G = [(\rho_p - \rho_f) g d^3]^{1/2} / \eta$, which compares gravity to fluid viscosity η effects (Fig. 3). Because grain inertia is not included in a static force balance, the gravity term is the only one involving particle density. A consequence is that the static threshold curve Θ_t vs G must be 'universal' in the sense that it is valid for any environment. Fig. 3 shows that 'static' curve, which fits subaqueous data of the literature. In the aeolian case, a dynamic model, which idealizes saltation by a typical grain trajectory, is needed to reproduce those threshold data, requiring an additional dimensionless parameter, the density ratio ρ_p / ρ_f . Fig. 3 gathers these data for sand grains with variable d in ambient conditions and our aeolian data with variable P and fixed grain size $d = 125 \mu\text{m}$, emphasizing the new regime, where the model fails.

Impact ripples: The origin of Martian ripples, exhibiting two distinct length scales, are currently

debated, see e.g. [8]. Here, we continuously observe the emergence of centimeter-scale impact ripples upon decreasing air pressure conditions (Fig. 4). Their characteristic wavelength and propagation velocity are essentially independent of pressure for a given value of the ratio u_*/u_t . This result can be understood in association with the existence of a surface collisional layer [9], and given the fact that the threshold $\rho_f u_t^2$ is roughly constant, to the first approximation. The slight increasing trend of the wavelength with pressure would need confirmation with additional experiments to reduce error bars on measurements.

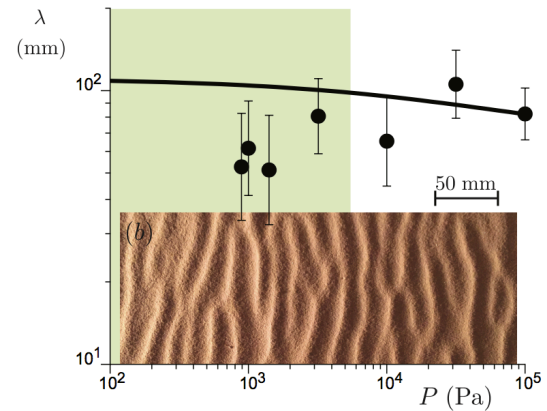


Fig. 4: Variation of ripple emergent wavelength with air pressure in the tunnel. Data: $u_*/u_t = 1.5$; Photo: $u_*/u_t = 1.1$ in Martian conditions.

All these findings challenge our fundamental understanding of sediment transport on planetary bodies and require further investigation. Novel ideas are required to explain the physical processes at work in this saltation regime reached at Galileo numbers orders of magnitude below well-known hydrodynamic transitions.

Acknowledgments: This work has been funded by Europlanet grant No 11376. Europlanet 2020 RI has received funding from the European Union's Horizon 2020 research and innovation program under grant agreement No 654208.

References: [1] Diniega S, et al. (2021) *Geomorphology* **380** 107627. [2] Durán Vinent O, Andreotti B, Claudin P, Winter C (2019) *Nature Geosci.* **12**, 345. [3] Jia P, Andreotti B, Claudin P (2017) *PNAS* **114**, 2509. [4] Andreotti B, Claudin P, Iversen JJ, Merrison JP, Rasmussen KR (2021) *PNAS* **118**, e2012386118. [5] Pätz T, et al. (2021) *JGR* **126**, e2020JF005859. [6] Greeley R, et al. (1980) *GRL* **7**, 121. [7] Swann C, Sherman D, Ewing R (2020) *GRL* **47**, e2019GL084484. [8] Lapôtre MGA, Ewing R, Lamb MP (2021) *JGR* **126**, e2020JE006729. [9] Durán O, Claudin P, Andreotti B (2014), *PNAS* **111**, 15665.